ORIGINAL RESEARCH

High-Content Screening Identifies Cyclosporin A as a Novel ABCA3-Specific Molecular Corrector

Maria Forstner[1]*, Sean Lin[2]*, Xiaohua Yang[1], Susanna Kinting[1], Ina Rothenaigner[2], Kenji Schorpp[2], Yang Li[1], Kamyar Hadian[2]‡, and Matthias Griese[1]‡

[1]Department of Pediatric Pneumology, Dr. von Hauner Children's Hospital–Ludwig-Maximilian University–German Center for Lung Research (DZL), Munich, Germany [2]Assay Development and Screening Platform, Institute of Molecular Toxicology and Pharmacology, German Research Center for Environmental Health, Neuherberg, Germany

ORCID ID: 0000-0002-1468-6969 (M.F.).

Abstract

ABCA3 (ATP-binding cassette subfamily A member 3) is a lipid transporter expressed in alveolar type II cells and localized in the limiting membrane of lamellar bodies. It is crucial for pulmonary surfactant storage and homeostasis. Mutations in the ABCA3 gene are the most common genetic cause of respiratory distress syndrome in mature newborns and of interstitial lung disease in children. Apart from lung transplant, there is no cure available. To address the lack of causal therapeutic options for ABCA3 deficiency, a rapid and reliable approach is needed to investigate variant-specific molecular mechanisms and to identify pharmacologic modulators for monotherapies or combination therapies. To this end, we developed a phenotypic cell-based assay to autonomously identify ABCA3 wild-type–like or mutant-like cells by using machine learning algorithms aimed at identifying morphologic differences in wild-type and mutant cells. The assay was subsequently used to identify new drug candidates for ABCA3-specific molecular correction by using high-content screening of 1,280 Food and Drug Administration–approved small molecules. Cyclosporin A was identified as a potent corrector, specific for some but not all ABCA3 variants. Results were validated by using our previously established functional small-format assays. Hence, cyclosporin A may be selected for orphan drug evaluation in controlled repurposing trials in patients.

Keywords: ABCA3; childhood interstitial lung disease; high-content screening; machine learning; cyclosporin A

The ABCA3 (ATP-binding cassette [ABC] transporter subfamily A member 3) protein is a phospholipid transporter in alveolar type II cells, which is essential for assembly and homeostasis of pulmonary surfactant and for lysosome-related lamellar body (LB) biogenesis, the storage compartment of surfactant (1–3). Localized to the LB-limiting membrane, ABCA3 hydrolyzes ATP to transport phosphatidylcholine and phosphatidylglycerol as major surfactant components into the LB (3–5). Biallelic ABCA3 variants (NM_001089.2) are the most common genetic cause of interstitial lung disease in children (6–9) and may also play a role in adult interstitial lung disease (10, 11). So far, only 10% of more than 200 described pathogenic ABCA3 variants were functionally classified (12–16). Nonsense and frameshift mutations result in a null phenotype with neonatal respiratory distress syndrome and death within the first months of life, whereas missense, in-frame insertions, deletions, or splicing variants may be

(Received in original form May 14, 2021; accepted in final form August 23, 2021)

*These authors contributed equally.

‡Co–senior authors

Supported by Deutsches Zentrum für Lungenforschung grant/award number FKZ82DZL23A2 (M.F.) and Friedrich-Baur-Stiftung grant/award number Reg.-Nr. 51/19 (M.F.).

Author Contributions: Conceptualization: M.F., S.L., K.H., and M.G. Investigation: M.F., S.L., X.Y., S.K., I.R., K.S., and Y.L. Formal analysis: M.F., S.L., X.Y., S.K., I.R., K.S., and Y.L. Project administration: M.F. and S.L. Writing (original draft): M.F., S.L., K.S., K.H., and M.G. Writing (review and editing): all authors.

Correspondence and requests for reprints should be addressed to Matthias Griese, M.D., Dr. von Haunersches Children's Hospital–Ludwig-Maximilian University, Lindwurmstraße 4, D-80337 Munich, Germany. E-mail: matthias.griese@med.uni-muenchen.de.

This article has a data supplement, which is accessible from this issue's table of contents at www.atsjournals.org.

Am J Respir Cell Mol Biol Vol ■■, Iss ■■, pp 1–9, ■■ ■■, 2021

Originally Published in Press as DOI: 10.1165/rcmb.2021-0223OC on ■■■
Internet address: www.atsjournals.org

compatible with survival (8, 9). Such variants either lead to misfolded ABCA3 proteins, abnormal intracellular trafficking, and retention in the endoplasmic reticulum (trafficking mutations) or lead to reduced ATP-mediated phospholipid transport (functional mutations) (12, 17–21). The resulting phenotypes are highly variable and difficult to predict (7, 22). Apart from lung transplant, no causal therapy is available for ABCA3-deficient patients (9, 23).

A probable approach to treating ABCA3-deficient patients might be modeled in analogy to the approach to treating patients with cystic fibrosis (CF). CF is caused by a mutant chloride channel, the CF transmembrane conductance regulator, which is another ABC transporter (i.e., ABCC7). Here, disease-causing mutants can be rescued by small molecules, which have revolutionized treatment (24–27). Recently, we and others have proven this concept *in vitro* for correctors and potentiators of trafficking and functional ABCA3 mutations, respectively (16, 28, 29). Yet a rapid and robust approach to investigating ABCA3 variant–specific molecular mechanisms and to identifying pharmacologic modulators and combinations of compounds is highly needed.

In this study, we developed a phenotypic cell-based assay that is compatible with high-content screening (HCS). We used the known ABCA3 corrector C13; the ABCA3 variant K1388N, a well-described clinically relevant trafficking mutation (13, 15, 28); and machine learning (ML) algorithms with the aim of unravelling ABCA3-specific correctors by screening a library of approved drugs. We identified cyclosporin A (CsA) and validated it as a potential corrector by using previously described functional small-format assays. In addition, we showed that CsA was able to correct several other mistrafficked ABCA3 variants by enabling ABCA3 maturation to wild-type (WT) levels. 10

Methods

Cell Culture/Treatment of Cells

A549 cells stably expressing WT or mutant HA-tagged ABCA3 protein (ABCA3-HA) were cultured, and stable cell clones were generated as previously described (13, 28).

IB, Immunofluorescence Staining, Confocal Microscopy, and TopFluor-labeled Phosphatidylcholine Transport Quantitation

Protein isolation, IB using 15 μg of total protein, TopFluor-labeled phosphatidylcholine (TopF-PC) transport quantitation, and immunofluorescence staining were performed as previously described (14, 28).

Screening Procedure

Plate and liquid handling were performed by using a multicomponent HTS platform. The procedure used for cell culture, the compound treatment of the cells, immunofluorescence staining, and imaging protocols are described in the data supplement.

Automated Image Analysis

Multiparametric image analysis was performed by using Columbus software version 2.8.0 (PerkinElmer). In the following, the analysis steps used in the Columbus software are described (*see* Figure E5 in the data supplement): GFP and Hoechst signals were smoothened by using median filters to reduce noise signals. Nuclei were detected via the Hoechst signal. The GFP channel was used to define the cytoplasm. In a next step, morphologic features (the area, roundness, width, length, and width-to-length ratio) and the intensity properties of the Hoechst and the GFP channels (the mean, SD, coefficient of variance, median, sum, maximum, minimum, and quantile fraction) were calculated for each cell region (the nuclei, cytoplasm, and whole cell). In addition, we calculated the texture properties for the whole cell for the GFP and Hoechst channels (SER features, Haralick features, and Gabor features). Moreover, we applied a filter to remove border objects (nuclei that cross image borders). We performed spot detection by using the GFP channel and again calculated the intensity (GFP signal) and morphologic properties of the spots. Next, we used the selection tool "Linear Classifier" (supervised classification task) to train the software to distinguish between A549 cells expressing mutant K1388N ("K1388N-like cells") and A549 cells expressing WT ABCA3-HA ("WT-like cells") (using all the properties we calculated before). For training, cells expressing K1388N (K1388N-like cells) and WT ABCA3-HA (WT-like cells) were manually selected. After training, the software calculates a classifier according to the linear model [$x = -\text{offset} + (\text{linear coefficient } 1 \times \text{property } 1) + (\text{linear coefficient } 2 \times \text{property } 2) + \cdots$] and identifies the linear combination of the most relevant properties that determines an effective discriminator for WT-like cells and K1388N-like cells. 14

For hit selection, a threshold of higher than 3 SDs from the median of the compound-treated population (percentage of WT-like cells) was set.

Viability Assay

For cell-viability experiments, the CellTiter-Glo 2.0 system (Promega) was used according to the manufacturer's manual. A549 cells stably expressing WT or K1388N ABCA3-HA were seeded in 384-well plates and treated with compounds in 10-point titrations (ranging from 500μM to 0.977μM). 15

Details about chemical correctors, the sample library, the texture properties used for supervised ML, and statistical analysis are described in the data supplement. 16 17

11

Results

Development of an HCS-Compatible Cell-based Assay for the Identification of ABCA3-Specific Small-Molecule Correctors

For the identification of molecular correctors of ABCA3 trafficking variants, we established an HCS-compatible robust phenotypic cell-based assay by optimizing various parameters, such as cell density and plate coating (Figures 1A and E1). When WT ABCA3-HA protein was co-localized with the lysosomal marker CD63 in LB-like vesicular structures, K1388N ABCA3-HA protein led to smaller vesicles accompanied by a diffuse pattern. ML analysis was used to recognize cells expressing WT (WT-like cells) and K1388N ABCA3-HA (K1388N-like cells) by evaluating and weighing differences in various morphologic features extracted from a training set of labeled immunofluorescence images (Figure 1B). 12 13 These relevant morphologic features allowed the ML algorithm to significantly discriminate between WT-like and K1388N-like cells (Figure 1C). To verify our established image-analysis routine, we used the compounds C13 and C17 as positive controls (Figure E1); these compounds have previously been shown to functionally rescue ABCA3 trafficking variants *in vitro* (16, 28).

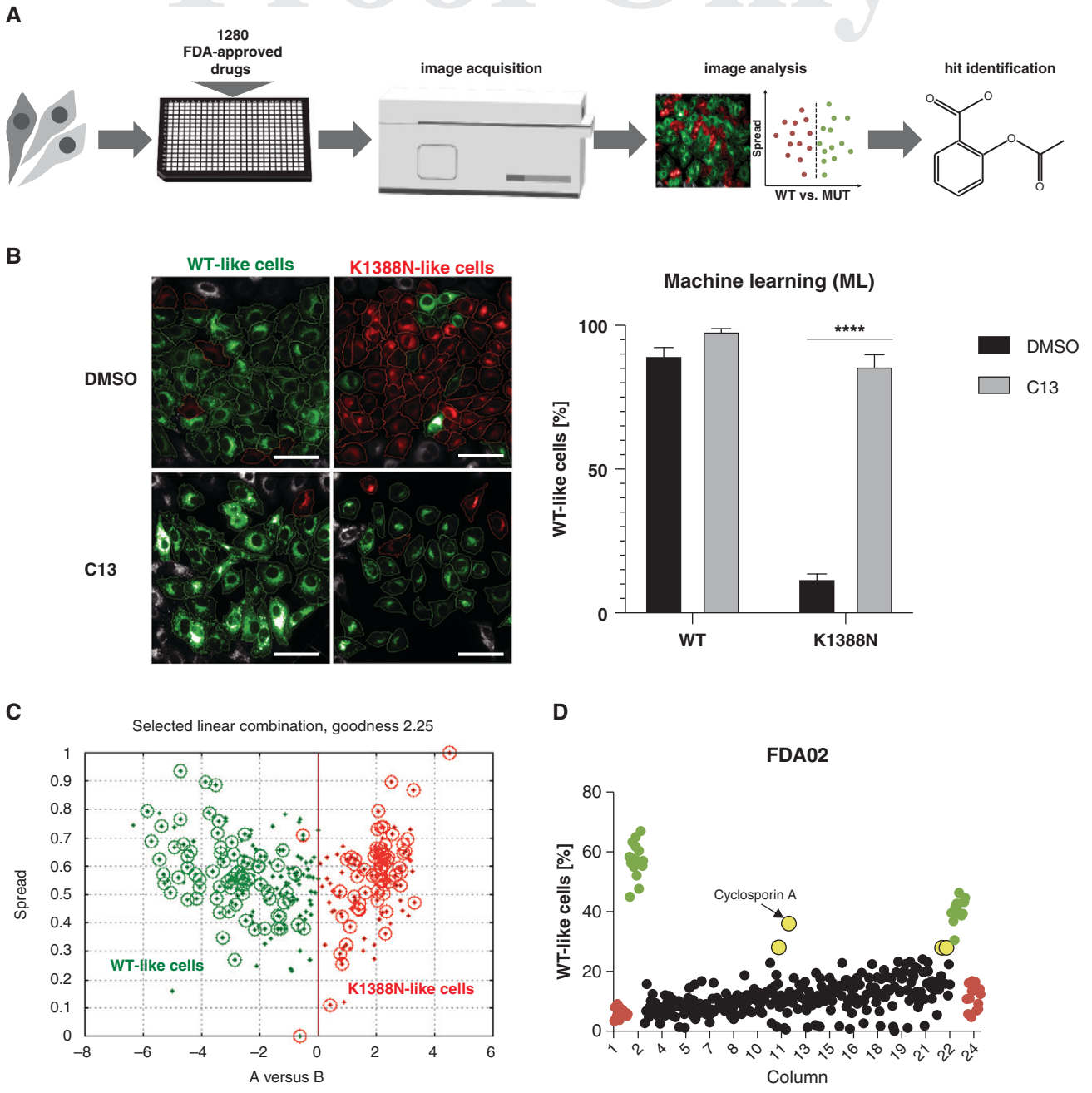

Figure 1. High-content screening of Food and Drug Administration (FDA)-approved, small-molecule ABCA3 (ATP-binding cassette subfamily A member 3) correctors. (*A*) Workflow of the high-content screening–compatible, cell-based phenotypic assay. The cells were seeded onto 384-well plates. After 24 hours, compounds were transferred and incubated for another 24 hours. The cells were then stained, fixed, and analyzed by using automated image analysis. Hits were analyzed by employing morphologic feature extraction coupled with a machine learning (ML) algorithm to determine the levels of "wild-type (WT)-like" and "K1388N-like" cells. (*B*) Validation of the multiparametric image analysis, which distinguishes between WT-like cells and K1388N-like cells by using an ML algorithm. Results were confirmed by using 10M C13, a previously described ABCA3 corrector. A549 cells stably expressing WT or mutant (MUT) K1388N HA-tagged ABCA3 protein (ABCA3-HA) were treated with 10M C13 for 24 hours and stained for ABCA3-HA. Representative images showing the subpopulations classified by the analysis (cells classified as WT-like are marked in green, and K1388N-like cells are marked in red). Scale bars, 20 m. Data are presented as the mean (SD) (mean of a well, $n = 16$). (*C*) Plot showing the optimized discrimination of WT-like versus K1388N-like cells by the analysis software after training of the system. Circled dots represent the cells used, and the color of each indicates the training class. The noncircled dots are the classified objects in the training images, and the color indicates the classification for that object. (*D*) Screening of 1,280 FDA-approved compounds on A549 cells expressing K1388N ABCA3-HA. Representative plot of one screening plate is shown. The ML results for WT-like cells (percentages) are sorted by the 24 columns of the screening plate. Hits are highlighted in yellow, including cyclosporin A (CsA). For hit selection, a threshold larger than 3 SDs from the median of the population was set. As negative controls, A549 cells expressing K1388N ABCA3-HA treated with 1% DMSO were used (left and right, orange). As positive controls, A549 cells expressing WT ABCA3-HA (left, green) and A549 cells expressing K1388N ABCA3-HA treated with 10M C13 corrector (right, green) were used.

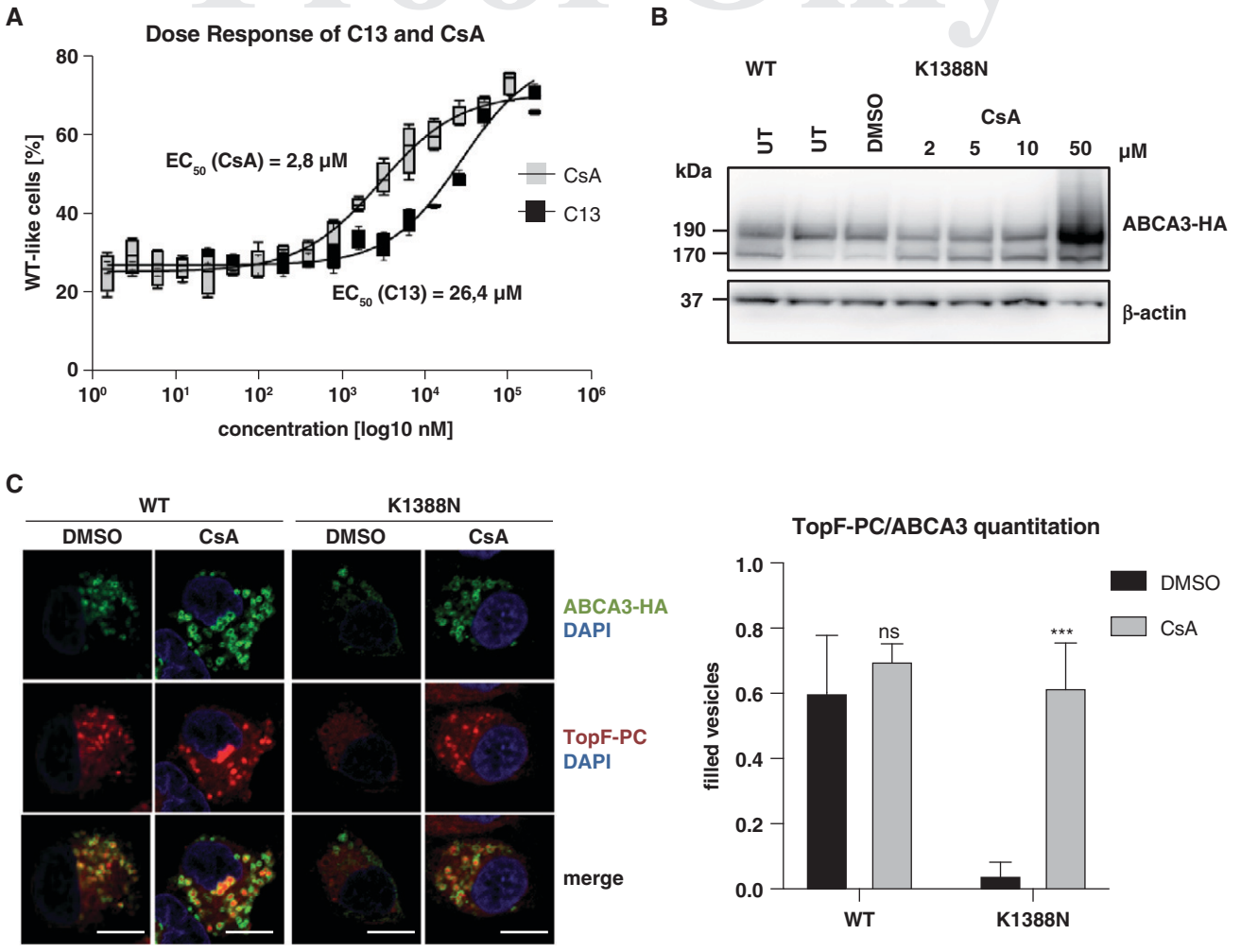

25 **Figure 2.** Validation of CsA as a drug correcting the ABCA3 variant K1388N. (*A*) Dose–response curves of cells expressing K1388N ABCA3-HA treated either with CsA or the corrector C13. WT-like cells quantified by using ML algorithms were plotted as percentages. Concentrations of CsA and C13 are shown at $\log_{10}$ scale in nanomolar units. The EC_{50} is displayed in micromolar units. Data are presented as the mean (SD) ($n = 4$). (*B*) A549 cells expressing K1388N ABCA3-HA were treated with increasing concentrations of CsA for 24 hours, and the ABCA3-HA protein pattern was analyzed by using Western blotting with an anti-HA antibody. Augmentation of the 170-kD band indicates restored processing of the protein. Results of the densitometric quantitation of the protein amount in each band (190 kD and 170 kD) are shown in the data supplement. (*C*) A549 cells expressing WT or K1388N ABCA3-HA were treated with 10M CsA for 24 hours, which was followed by incubation with liposomes containing TopFluor-labeled phosphatidylcholine (TopF-PC) and treatment with 10M CsA for another 24 hours. The portion of TopF-PC–filled $ABCA3^+$ vesicles was measured. Representative images of the experiment show restored TopF-PC–filled $ABCA3^+$ vesicles of the ABCA3-HA variant K1388N upon CsA treatment. Scale bars, 10 m. Pseudocolors were used, which is consistent with former experiments. Three independent experiments were performed. Results are the mean + SEM. $^{***}P < 0.001$. EC_{50} = half-maximal effective concentration; ns = not significant; UT = untreated.

26

The ML algorithm was able to reliably classify ~86% of C13-incubated cells expressing K1388N ABCA3-HA as WT-like cells (Figure 1B).

Identification of Hit Compounds in a Library of 1,280 Food and Drug Administration–approved Small-Molecule Drugs

18 Next, we screened a library of Food and
19 Drug Administration (FDA)-approved small-molecule compounds at a fixed concentration of 10µM (Figure 1D). The screening assay quality was determined by Z'-factor calculation. Compounds were defined as hits if they increased the percentage of WT-like cells per well of treated K1388N ABCA3-HA mutant by a number greater than 3 SDs over the median value of the compound-treated population. Calculation of the Z' factor and the signal window showed excellent screening performance (Figure E1D and data not shown). The screening resulted in 12 hit compounds (Figure E2A), which were further analyzed. For hit validation, the ratio 20
of cleaved-to-uncleaved ABCA3 was analyzed by using Western blotting. The detection of uncleaved (190 kD) and cleaved (170 kD) ABCA3 protein served as semiquantitative markers for the identification of ABCA3 trafficking variants. ABCA3 proteins are retained in the

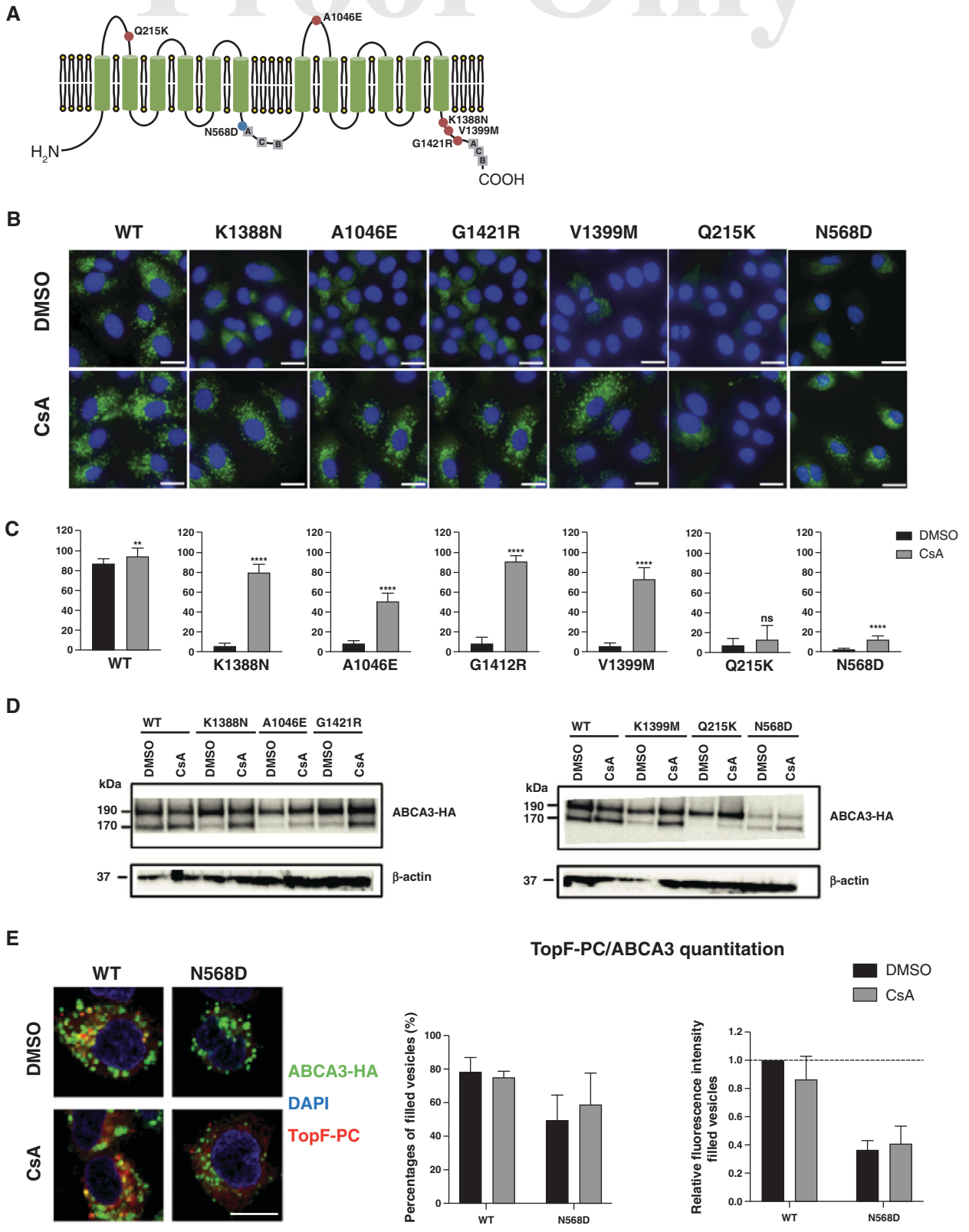

Figure 3. CsA corrected other ABCA3-HA variants. (*A*) The positions of all ABCA3-HA variants tested in this study were marked in the topology model. Trafficking mutations with abnormal intracellular trafficking of the transporter are marked in red, whereas the functional mutation N568D is marked in blue. (*B*) Representative images of the mutations after 24 hours of treatment with 10M CsA or the DMSO control are shown. WT and MUT ABCA3-HA cells were stained against anti-HA. Hoechst was used for nuclear staining. Images were obtained by using a high-content

27

endoplasmic reticulum and fail to be glycosylated and proteolytically processed in Golgi and post-Golgi compartments. Consequently, K1388N ABCA3-HA resulted in a markedly decreased 170/190–kD ratio (28). To verify the hit compounds, we acquired the 12 hits from independent stocks and treated A549 cells expressing K1388N ABCA3-HA with these hit compounds. The protein level of the processed 170-kD ABCA3 species was increased by four hit compounds, confirming their corrector capacity. Clomipramine hydrochloride (CLI), CsA, doxazosin mesylate (DZN), and *R*-duloxetine hydrochloride (DX) had strong effects on the ratio of cleaved-to-uncleaved ABCA3 (Figure E2B). Consistent with the decrease in cleaved-to-uncleaved ABCA3, treatment of the cells with CLI, CsA, DZN, and DX restored the subcellular localization of K1388N ABCA3-HA in immunofluorescence assays, displaying lysosome-related (anti-CD63) vesicle-like structures as seen in cells expressing WT ABCA3-HA, which indicates restored LB morphology (Figure E2C). In parallel, dose-dependent toxicity of the hit compounds was assessed via a cell-viability assay. Ten-point titrations showed high toxicity to the cells for 7 of the 12 hit compounds (pyrvinium pamoate, IVE, DX, DZN, CLI, epiandrosterone, and mitoxantrone hydrochloride); those compounds were therefore excluded from further experiments (Figure E2D). Altogether, CsA was the most potent corrector with drug-like properties in the initial screening as well as in the follow-up verification and showed no cellular toxicity. Importantly, CsA is broadly used for other indications in children (30–33) and was thus further evaluated.

Validation of CsA as a Molecular Corrector for ABCA3 Trafficking Mutants

CsA dose-dependently increased the number of cells that were classified as WT-like in K1388N ABCA3-HA–expressing cells, demonstrating a half-maximal effective concentration of 2.8μM. For comparison, the half-maximal effective concentration of the established corrector C13 was 26.4μM (Figure 2A). On the protein level, increasing doses of CsA led to an elevated level of the processed 170-kD ABCA3-HA species and thereby raised the 170/190–kD ratio of K1388N ABCA3-HA (Figures 2B and E3A). The quantitation of TopF-PC transport served as a functional assay for ABCA3 activity (14). CsA significantly increased the function of K1388N ABCA3-HA, as demonstrated by similar ratios of TopF-PC–filled vesicles in WT and mutant ABCA3-HA cells after treatment (Figure 2C).To test the broader applicability of CsA, we evaluated its effect on a larger set of trafficking mutants and one functional mutant (Figure 3A). We applied ML to distinguish A549 cells expressing WT ABCA3-HA from cells either expressing the trafficking mutant K1388N ABCA3-HA or the functional mutant N568D ABCA3-HA. We were successful in distinguishing A549 cells expressing ABCA3-variant N568D from the trafficking mutant in their cellular morphology (Figures E4A and E4B). Notably, CsA corrected the K1388N, A1046E, G1421R, and V1399M ABCA3-HA trafficking mutants to levels of 50% to beyond 90% of WT-like cells. However, the trafficking mutant Q215K was not responsive to CsA treatment (Figures 3B and 3C). CsA treatment of cells expressing the functional mutant N568D ABCA3-HA only showed a marginal increase in the percentage of WT-like cells (Figures 3B and 3C). We further confirmed the imaging-based results by using Western blotting to analyze protein expression levels (Figures 3D and E3B). Here, only the trafficking mutants K1388N, A1046E, G1421R, and V1399M ABCA3-HA demonstrated an effect. In addition, we showed that the functionality of the N568D ABCA3 protein was not increased, as shown by similar percentages of TopF-PC–filled $ABCA3^+$ vesicles and similar relative fluorescence intensity/TopF-PC–filled vesicles upon treatment with DMSO or CsA (Figure 3E).

Potential Mode of Action of CsA on ABCA3

CsA inhibits calcineurin by forming a complex with cyclophilin A and acts via calcineurin-independent pathways by inhibiting cyclophilins (34–36). To unravel which of the above-mentioned inhibitory pathways of CsA is able to correct ABCA3 variants, we exposed A549 cells expressing K1388N ABCA3-HA to the calcineurin inhibitor pimecrolimus (37) alone, the cyclophilin inhibitor NIM811 (38) alone, or the combination of the two. Monotreatment with pimecrolimus or NIM811 resulted in partial rescue of the ABCA3 K1883N-HA–induced trafficking phenotype (Figure 4B) and an increase in processed ABCA3 species (Figure 4C). The combinatorial treatment of pimecrolimus and NIM811 reverted the trafficking ABCA3 mutant variant phenotype to a comparable level seen with the treatment of CsA (Figure 4B), although results were less pronounced than in Western blotting assays (Figure 4C). Together, the individual and synergistic effects of pimecrolimus and NIM811 suggests that CsA uses calcineurin-dependent as well as calcineurin-independent pathways to correct ABCA3.

21

Discussion

The purpose of this study was to develop a phenotypic high-content screen to identify small-molecule correctors for patients suffering from ABCA3 deficiency and to perform a screen of a library of FDA-approved compounds. We identified 12 hit candidates and evaluated them in conventional assays. CsA was the most promising hit and is a well-known drug that has been safely used in children for decades. Yet adverse effects, including

Figure 3. (*continued*) imaging system. Scale bars, 10 m. (*C*) Quantitative measurements of ABCA3 trafficking MUTs and the functional MUT N568D upon 10M CsA or DMSO treatment for 24 hours. WT-like cells quantified by using ML algorithms are plotted as percentages. Data are presented as the mean (SD) ($n = 16$). $^{**}P < 0.01$ and $^{****}P < 0.0001$. (*D*) A549 cells expressing A1046E, G1421R, V1399M, Q215K, and N568D ABCA3-HA were treated with 10M CsA for 24 hours, and the ABCA3-HA protein pattern was analyzed by using Western blotting with an anti-HA antibody. Augmentation of the 170-kD band indicates restored processing of the protein. Results of the densitometric quantitation of the protein amount in each band (190 kD and 170 kD) are shown in the data supplement. (*E*) A549 cells expressing WT or N568D ABCA3-HA were incubated with liposomes containing TopF-PC and treated with 10M CsA for 24 hours. Representative images of the experiment show a smaller number of TopF-PC–filled $ABCA3^+$ vesicles of the ABCA3-HA variant N568D. The portion of TopF-PC–filled $ABCA3^+$ vesicles and the relative fluorescence intensity/filled vesicles were measured upon treatment with CsA. Scale bar, 10 m. Pseudocolors were used, which is consistent with former experiments. Four independent experiments were performed. Results are the mean + SEM.

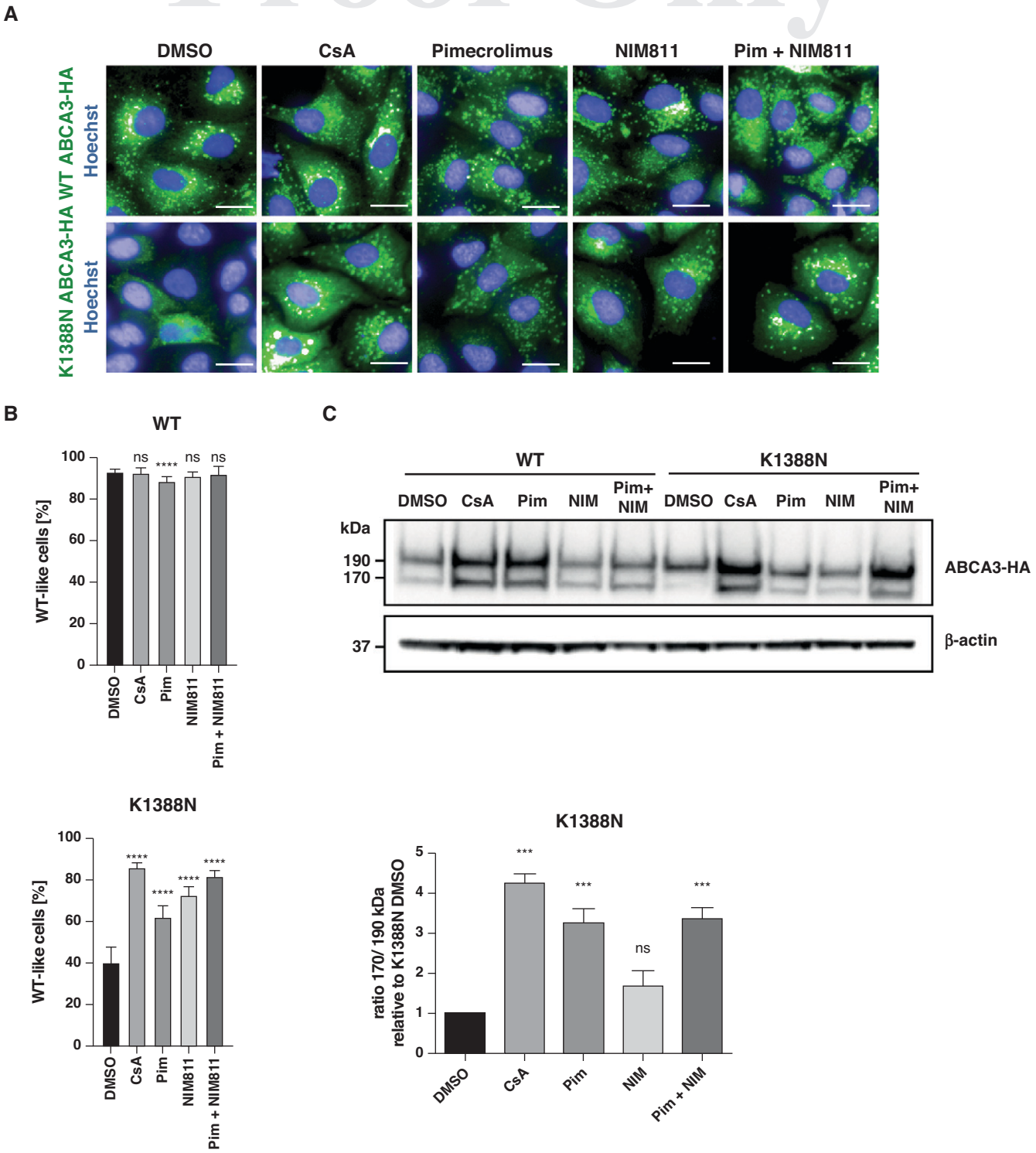

Figure 4. Treatment with pimecrolimus (Pim) and NIM811 (NIM) restored processing of K1388N ABCA3-HA. (*A*) A549 cells expressing WT or K1388N ABCA3-HA were treated with 10M CsA, 5M Pim, 2M NIM, and the combination of 5M Pim and 2M NIM for 24 hours. Representative images of cells stained for ABCA3-HA localization and Hoechst are shown. Scale bar, 20 m. (*B*) Quantitative analysis of WT-like cells of cells expressing either WT or K1388N ABCA3-HA by using ML algorithms that allow the recognition. Data are presented as the mean (SD) ($n = 16$). ****$P < 0.0001$. (*C*) The ABCA3-HA protein pattern was analyzed by using Western blotting. Augmentation of the 170-kD band indicates restored processing of the protein. Densitometric quantitation of the protein amount in each band (190 kD and 170 kD) was performed by using ImageJ software, and the ratio of 170 kD to 190 kD bands was calculated by using DMSO-treated K1388N set to 1. Results are the mean + SEM of four independent experiments. ***$P < 0.001$ regarding the DMSO vehicle control.

immunosuppression, impairment of renal function, and increased blood pressure, have to be taken in account. Blood-level monitoring is routine in clinical usage of CsA (31–33, 39).

Importantly, by using a linear classifier and training data with labeled images, we not only were able to differentiate WT from mutant cells expressing either WT or the mutant K1388N ABCA3 but were also able to significantly demonstrate and confirm the corrective effect of C13 on K1388N cells (16, 28). Thus, the screening approach should allow for the identification of molecules with an effect comparable with or even better than that of C13. Our initial screen hit rate was 0.9%. Retesting of hit compounds from reordered stocks confirmed selected candidates in the conventional experimental setup. Our phenotypic assay helped us to discover corrective compounds without the detailed characterization of the mechanism of a mutation. Here, our ML-based analysis strategy used various features like textures, intensity, and morphology to classify WT- and mutant-like cells, thus not relying on a detailed molecular understanding of the ABCA3 mutation biology. This is particularly beneficial for testing novel compounds on a large set of newly discovered mutants. Importantly, we have established an assay/analysis pipeline that will distinguish among WT ABCA3, trafficking mutations, and functional mutations, which is a valuable resource for future small-molecule discovery to identify ABCA3 potentiators/correctors. The production of cell lines stably expressing newly discovered variants for compound testing could efficiently be accomplished by using the landing-pad system (16) with the aligned degree of ABCA3 expression.

CsA corrected trafficking of K1388N, A1046E, G1421R, and V1399M mutants. However, Q215K, another trafficking variant, was not responsive to CsA (Figure 3). This variant was also not as susceptible to correction by C13, indicating that this variant might have secondary defects that are not affected by CsA or C13. In line with that, CsA did not improve the transport function of ABCA3 in the functional mutant N568D. CsA was shown to correct trafficking mutants of ABCB4 and ABCB1 in several cell models, depending on the underlying variant (40–45). In those studies, evidence was obtained that CsA led to an improved correction of the mutants through its chaperone abilities, which may be a mechanism also involved in ABCA3 correction, although this needs further validation. In this study, we tested the participation of calcineurin and cyclophilin inhibition in ABCA3-specific correction, and their contribution is supported by our results using pimecrolimus and NIM811 (37, 38). The synergistic effect of pimecrolimus and NIM811 suggests that CsA uses calcineurin and calcineurin-independent pathways to correct ABCA3. These and additional mechanisms, including repression of the transcription of mutant ABCA3 protein via reduced NFAT3 signaling through calcineurin inhibition, as suggested by Davé and colleagues (46), will be a matter of further investigation.

Limitations of the A549 cell model are that it does not account for the patient-specific genetic or environmental background and that only homozygous mutations can be assessed. In addition, the impact of ABCA3 overexpression is not scalable. To allow for comparisons between WT ABCA3 and different variants, we carefully aligned ABCA3 expression in all stable lines that we generated. These limitations may be overcome with patient-derived induced pluripotent stem cells in future studies (47, 48).

ABCA3 deficiency is a rare clinical condition (8), making conventional clinical studies difficult to conduct. Therefore, the screening of FDA-approved drugs and assessment of their clinical value in trials may provide an intermediate step toward urgently needed treatments. Repurposing studies have the potential to bridge the time necessary for the development of new molecules, which still have a high rate of failure and may require many years of development before patients benefit (49, 50). Hence, CsA, identified in this work, may be a candidate treatment option in ABCA3 deficiency, depending on the responsiveness of the underlying mutation. ■

Author disclosures are available with the text of this article at www.atsjournals.org.

Acknowledgment: The authors thank Stefanie Brandner for excellent technical assistance.

References

1. Whitsett JA, Wert SE, Weaver TE. Alveolar surfactant homeostasis and the pathogenesis of pulmonary disease. *Annu Rev Med* 2010;61: 105–119.
2. Weaver TE, Na CL, Stahlman M. Biogenesis of lamellar bodies, lysosome-related organelles involved in storage and secretion of pulmonary surfactant. *Semin Cell Dev Biol* 2002;13:263–270.
3. Ban N, Matsumura Y, Sakai H, Takanezawa Y, Sasaki M, Arai H, *et al.* ABCA3 as a lipid transporter in pulmonary surfactant biogenesis. *J Biol Chem* 2007;282:9628–9634.
4. Yamano G, Funahashi H, Kawanami O, Zhao LX, Ban N, Uchida Y, *et al.* ABCA3 is a lamellar body membrane protein in human lung alveolar type II cells. *FEBS Lett* 2001;508:221–225.
5. Mulugeta S, Gray JM, Notarfrancesco KL, Gonzales LW, Koval M, Feinstein SI, *et al.* Identification of LBM180, a lamellar body limiting membrane protein of alveolar type II cells, as the ABC transporter protein ABCA3. *J Biol Chem* 2002;277:22147–22155.
6. Shulenin S, Nogee LM, Annilo T, Wert SE, Whitsett JA, Dean M. ABCA3 gene mutations in newborns with fatal surfactant deficiency. *N Engl J Med* 2004;350:1296–1303.
7. Doan ML, Guillerman RP, Dishop MK, Nogee LM, Langston C, Mallory GB, *et al.* Clinical, radiological and pathological features of ABCA3 mutations in children. *Thorax* 2008;63:366–373.
8. Wambach JA, Casey AM, Fishman MP, Wegner DJ, Wert SE, Cole FS, *et al.* Genotype-phenotype correlations for infants and children with ABCA3 deficiency. *Am J Respir Crit Care Med* 2014;189:1538–1543.
9. Kröner C, Wittmann T, Reu S, Teusch V, Klemme M, Rauch D, *et al.* Lung disease caused by *ABCA3* mutations. *Thorax* 2017;72:213–220.
10. Manali ED, Legendre M, Nathan N, Kannengiesser C, Coulomb-L'Hermine A, Tsiligiannis T, *et al.* Bi-allelic missense *ABCA3* mutations in a patient with childhood ILD who reached adulthood. *ERJ Open Res* 2019;5:00066-2019.
11. Klay D, Platenburg MGJP, van Rijswijk RHNAJ, Grutters JC, van Moorsel CHM. ABCA3 mutations in adult pulmonary fibrosis patients: a case series and review of literature. *Curr Opin Pulm Med* 2020;26:293–301.
12. Weichert N, Kaltenborn E, Hector A, Woischnik M, Schams A, Holzinger A, *et al.* Some ABCA3 mutations elevate ER stress and initiate apoptosis of lung epithelial cells. *Respir Res* 2011;12:4.
13. Wittmann T, Schindlbeck U, Höppner S, Kinting S, Frixel S, Kröner C, *et al.* Tools to explore ABCA3 mutations causing interstitial lung disease. *Pediatr Pulmonol* 2016;51:1284–1294.

14. Höppner S, Kinting S, Torrano AA, Schindlbeck U, Bräuchle C, Zarbock R, *et al.* Quantification of volume and lipid filling of intracellular vesicles carrying the ABCA3 transporter. *Biochim Biophys Acta Mol Cell Res* 2017;1864:2330–2335.
15. Schindlbeck U, Wittmann T, Höppner S, Kinting S, Liebisch G, Hegermann J, *et al.* ABCA3 missense mutations causing surfactant dysfunction disorders have distinct cellular phenotypes. *Hum Mutat* 2018;39:841–850.
16. Wambach JA, Yang P, Wegner DJ, Heins HB, Luke C, Li F, *et al.* Functional genomics of *ABCA3* variants. *Am J Respir Cell Mol Biol* 2020;63:436–443.
17. Matsumura Y, Ban N, Ueda K, Inagaki N. Characterization and classification of ATP-binding cassette transporter ABCA3 mutants in fatal surfactant deficiency. *J Biol Chem* 2006;281:34503–34514.
18. Cheong N, Madesh M, Gonzales LW, Zhao M, Yu K, Ballard PL, *et al.* Functional and trafficking defects in ATP binding cassette A3 mutants associated with respiratory distress syndrome. *J Biol Chem* 2006;281: 9791–9800.
19. Matsumura Y, Ban N, Inagaki N. Aberrant catalytic cycle and impaired lipid transport into intracellular vesicles in ABCA3 mutants associated with nonfatal pediatric interstitial lung disease. *Am J Physiol Lung Cell Mol Physiol* 2008;295:L698–L707.
20. Wambach JA, Yang P, Wegner DJ, Heins HB, Kaliberova LN, Kaliberov SA, *et al.* Functional characterization of ATP-binding cassette transporter A3 mutations from infants with respiratory distress syndrome. *Am J Respir Cell Mol Biol* 2016;55:716–721.
21. Beers MF, Mulugeta S. The biology of the ABCA3 lipid transporter in lung health and disease. *Cell Tissue Res* 2017;367:481–493.
22. Bullard JE, Wert SE, Nogee LM. ABCA3 deficiency: neonatal respiratory failure and interstitial lung disease. *Semin Perinatol* 2006;30:327–334.
23. Eldridge WB, Zhang Q, Faro A, Sweet SC, Eghtesady P, Hamvas A, *et al.* Outcomes of lung transplantation for infants and children with genetic disorders of surfactant metabolism. *J Pediatr* 2017;184:157–164, e2.
24. Galietta LV, Jayaraman S, Verkman AS. Cell-based assay for high-throughput quantitative screening of CFTR chloride transport agonists. *Am J Physiol Cell Physiol* 2001;281:C1734–C1742.
25. Pedemonte N, Lukacs GL, Du K, Caci E, Zegarra-Moran O, Galietta LJ, *et al.* Small-molecule correctors of defective DeltaF508-CFTR cellular processing identified by high-throughput screening. *J Clin Invest* 2005; 115:2564–2571.
26. Solomon GM, Marshall SG, Ramsey BW, Rowe SM. Breakthrough therapies: cystic fibrosis (CF) potentiators and correctors. *Pediatr Pulmonol* 2015;50:S3–S13.
27. Van Goor F, Straley KS, Cao D, González J, Hadida S, Hazlewood A, *et al.* Rescue of ΔF508-CFTR trafficking and gating in human cystic fibrosis airway primary cultures by small molecules. *Am J Physiol Lung Cell Mol Physiol* 2006;290:L1117–L1130.
28. Kinting S, Höppner S, Schindlbeck U, Forstner ME, Harfst J, Wittmann T, *et al.* Functional rescue of misfolding ABCA3 mutations by small molecular correctors. *Hum Mol Genet* 2018;27:943–953.
29. Kinting S, Li Y, Forstner M, Delhommel F, Sattler M, Griese M. Potentiation of ABCA3 lipid transport function by ivacaftor and genistein. *J Cell Mol Med* 2019;23:5225–5234.
30. Hoyer PF; Neoral Pediatric Study Group. Cyclosporin a (neoral) in pediatric organ transplantation. *Pediatr Transplant* 1998;2:35–39.
31. Saracco P, Quarello P, Iori AP, Zecca M, Longoni D, Svahn J, *et al.*; Bone Marrow Failure Study Group of the AIEOP (Italian Association of Paediatric Haematology Oncology). Cyclosporin A response and dependence in children with acquired aplastic anaemia: a multicentre retrospective study with long-term observation follow-up. *Br J Haematol* 2008;140:197–205.
32. Henriques LdosS, Matos FdeM, Vaisbich MH. Pharmacokinetics of cyclosporin–a microemulsion in children with idiopathic nephrotic syndrome. *Clinics (São Paulo)* 2012;67:1197–1202.
33. Liu AP, Cheuk DK, Lee AH, Lee PP, Chiang AK, Ha SY, *et al.* Cyclosporin A for persistent or chronic immune thrombocytopenia in children. *Ann Hematol* 2016;95:1881–1886.
34. Liu J, Farmer JD Jr, Lane WS, Friedman J, Weissman I, Schreiber SL. Calcineurin is a common target of cyclophilin-cyclosporin A and FKBP-FK506 complexes. *Cell* 1991;66:807–815.
35. Ram BM, Ramakrishna G. Endoplasmic reticulum vacuolation and unfolded protein response leading to paraptosis like cell death in cyclosporine A treated cancer cervix cells is mediated by cyclophilin B inhibition. *Biochim Biophys Acta* 2014;1843:2497–2512.
36. Schreiber SL, Crabtree GR. The mechanism of action of cyclosporin A and FK506. *Immunol Today* 1992;13:136–142.
37. Grassberger M, Baumruker T, Enz A, Hiestand P, Hultsch T, Kalthoff F, *et al.* A novel anti-inflammatory drug, SDZ ASM 981, for the treatment of skin diseases: *in vitro* pharmacology. *Br J Dermatol* 1999;141:264–273.
38. Billich A, Hammerschmid F, Peichl P, Wenger R, Zenke G, Quesniaux V, *et al.* Mode of action of SDZ NIM 811, a nonimmunosuppressive cyclosporin A analog with activity against human immunodeficiency virus (HIV) type 1: interference with HIV protein-cyclophilin A interactions. *J Virol* 1995;69:2451–2461.
39. Cooney GF, Habucky K, Hoppu K. Cyclosporin pharmacokinetics in paediatric transplant recipients. *Clin Pharmacokinet* 1997;32: 481–495.
40. Andress EJ, Nicolaou M, Romero MR, Naik S, Dixon PH, Williamson C, *et al.* Molecular mechanistic explanation for the spectrum of cholestatic disease caused by the S320F variant of ABCB4. *Hepatology* 2014;59: 1921–1931.
41. Delaunay JL, Durand-Schneider AM, Dossier C, Falguières T, Gautherot J, Davit-Spraul A, *et al.* A functional classification of ABCB4 variations causing progressive familial intrahepatic cholestasis type 3. *Hepatology* 2016;63:1620–1631.
42. Gautherot J, Durand-Schneider AM, Delautier D, Delaunay JL, Rada A, Gabillet J, *et al.* Effects of cellular, chemical, and pharmacological chaperones on the rescue of a trafficking-defective mutant of the ATP-binding cassette transporter proteins ABCB1/ABCB4. *J Biol Chem* 2012;287:5070–5078.
43. Kapoor K, Bhatnagar J, Chufan EE, Ambudkar SV. Mutations in intracellular loops 1 and 3 lead to misfolding of human P-glycoprotein (ABCB1) that can be rescued by cyclosporine A, which reduces its association with chaperone Hsp70. *J Biol Chem* 2013;288:32622–32636.
44. Loo TW, Clarke DM. Correction of defective protein kinesis of human P-glycoprotein mutants by substrates and modulators. *J Biol Chem* 1997;272:709–712.
45. Park HJ, Kim TH, Kim SW, Noh SH, Cho KJ, Choi C, *et al.* Functional characterization of ABCB4 mutations found in progressive familial intrahepatic cholestasis type 3. *Sci Rep* 2016;6:26872.
46. Davé V, Childs T, Xu Y, Ikegami M, Besnard V, Maeda Y, *et al.* Calcineurin/Nfat signaling is required for perinatal lung maturation and function. *J Clin Invest* 2006;116:2597–2609.
47. Merkert S, Schubert M, Olmer R, Engels L, Radetzki S, Veltman M, *et al.* High-throughput screening for modulators of CFTR activity based on genetically engineered cystic fibrosis disease-specific IPSCS. *Stem Cell Reports* 2019;12:1389–1403.
48. Jacob A, Morley M, Hawkins F, McCauley KB, Jean JC, Heins H, *et al.* Differentiation of human pluripotent stem cells into functional lung alveolar epithelial cells. *Cell Stem Cell* 2017;21:472–488, e10.
49. Pushpakom S, Iorio F, Eyers PA, Escott KJ, Hopper S, Wells A, *et al.* Drug repurposing: progress, challenges and recommendations. *Nat Rev Drug Discov* 2019;18:41–58.
50. Hoolachan JM, Sutton ER, Bowerman M. Teaching an old drug new tricks: repositioning strategies for spinal muscular atrophy. *Future Neurol* 2019;14:FNL25.

AUTHOR QUERIES

QA1 If you provided an ORCID ID at submission, please confirm that it appears correctly on the opening page of this article.

QA2 Please confirm that all necessary grants and funding sources are mentioned in the support footnote.

1 Any variations in capitalization and/or italics in genetic nomenclature have been retained per the original manuscript. Please confirm that all nomenclature has been formatted properly throughout. Per journal style, gene and protein symbols should be explained parenthetically after the symbol and defined in figures and table legends. However, if a gene/protein is mentioned in passing or is peripheral to the main point/discussion, it is not necessary to add an explanation. Also, these symbols may be retained even if used only once, and they do not need to be defined in titles. Please verify appropriate use throughout.

2 Please check article carefully throughout to verify that edits for grammar and clarity have preserved your intent.

3 Please confirm that all figures and tables are original to this manuscript and have not previously appeared elsewhere in any print or electronic form (including the Internet). If they have appeared elsewhere, please provide the reference of the source, as well as confirmation that written permission to reprint (or reprint with modifications) has been received (or that the original is in the public domain). If the original is an ATS publication, permission is automatically granted.

4 Please confirm presentation of partnered institutions in affiliation 1.

5 Per journal style, each affiliation may appear in either English or the language spoken at the location of the affiliation. However, each affiliation should be entirely in one language. Please verify edits to affiliation 2 or correct as necessary.

6 Please check slashes throughout and replace with "and", "or", or "and/or" if appropriate.

7 The footnote indicating M.F.'s funding has been changed to a financial support statement per journal style. Please confirm that edits to wording and format preserve your intent.

8 Please confirm that edits to the Author Contributions footnote preserve your intent. Information about equal contribution has been removed, as this information is included in footnote *.

9 The institutional information in the correspondence footnote has been edited to more closely match the corresponding author's affiliation and the information provided at submission. Please confirm or amend.

10 Per journal style, "concentration(s)," "amount(s)," and "degree(s)" are preferred to "level(s)" when applicable. Please amend throughout as appropriate.

11 Per journal style, in-text supplement citations have been designated with an "E" before the number; please amend the supplement accordingly and send corrected files (with a note detailing the changes that were made) to Ms. Mary Mobley (mmobley@thoracic.org).

12 Please spell out SER at only use in main text.

13 Please provide the manufacturer for product "Linear Classifier" in main text.

14 Please verify styling of mathematical terms and symbols in text and equations throughout article to ensure they appear correctly. Check carefully for correct use of boldface, italics, operators, qualifiers, spacing, superscripts, and subscripts.

15 In the sentence beginning "A549 cells stably expressing WT or K1388N ABCA3-HA were seeded … " in main text, please confirm the range of titrations ("500M to 0.977M"). Should the larger value be listed last, or was "0.977M" intended to be "977M"? Please amend if needed.

16 Units of molar concentration have been closed up to the number throughout as per AMA style. Please confirm or amend.

17 Commas and decimal points in numbers have been edited per American style; please check throughout and verify accuracy.

18 Please confirm expansion of FDA in the heading beginning "Identification of Hit Compounds … " in main text.

19 Please confirm added definition for FDA at first use in main text outside of a heading.

20 Please confirm replacement of apostrophes with prime symbols in "Z(factor" throughout. Please also confirm that "Z" should be italicized.

21 Please confirm expansion of WB at only use in main text.

22 Journal style is to define all abbreviations used in figure artwork and figure legends at the first occurrence. If an abbreviation is defined in Figure 1, we do not need to define it again in the remaining figure legends. Please verify that this style has been followed.

23 Please confirm added definition for FDA in the Figure 1 legend.

24 Please confirm added definition for MUT in the Figure 1 legend.

25 In Figure 1, **** appears in the figure but is not explained in the legend; please add an explanation.

26 Please confirm added definition for ns at the end of the Figure 2 legend.

27 In the Figure 3 and 4 legends, please add a noun after Hoechst if needed for clarity.